Optimal trajectories of electric sail with uncertainties

Andrea Caruso*, Lorenzo Niccolai†, Giovanni Mengali‡ and Alessandro A. Quarta§
University of Pisa, Pisa, Italy, 56122

An Electric Solar Wind Sail (E-sail) is an innovative propellantless propulsion system that generates a propulsive acceleration by exchanging momentum with the solar wind charged particles. Optimal E-sail trajectories are usually investigated by assuming an average value of the solar wind characteristics, thus obtaining a deterministic reference trajectory. However, recent analyses have shown that the solar wind dynamic pressure should be modelled as a random variable and an E-sail-based spacecraft may hardly be steered toward a target celestial body in an uncertain environment with just an open-loop control law. Therefore, this paper proposes to solve such a problem with a combined control strategy that suitably adjusts the grid electric voltage in response to the measured value of the dynamic pressure, and counteracts the effects of the solar wind uncertainties by rectifying the nominal trajectory at suitably chosen points. The effectiveness of such an approach is verified by simulation using two-dimensional transfer scenarios.

Nomenclature

$\boldsymbol{a}$	=	propulsive acceleration vector, (mm/s^2)
a_c	=	characteristic acceleration, (mm/s^2)
a_r	=	radial propulsive acceleration, (mm/s^2)
a_θ	=	circumferential propulsive acceleration, (mm/s^2)
e	=	eccentricity
$\mathcal{H}$	=	Hamiltonian function
J	=	performance index
L	=	tether length, (km)
m	=	spacecraft mass, (kg)
N	=	number of tethers
$\hat{\boldsymbol{n}}$	=	unit vector normal to the E-sail plane
O	=	Sun's center-of-mass
p	=	semilatus rectum, (au)
$p_\oplus$	=	solar wind dynamic pressure at 1 au, (nPa)
r	=	Sun-spacecraft distance, (au)
$r_\oplus$	=	Sun-Earth distance (1 au)
$\hat{\boldsymbol{r}}$	=	radial unit vector
$\mathcal{T}$	=	polar reference frame
t	=	time, (days)
$t^{\mathrm{d}}_{\mathrm{end}}$	=	final time along the deviation arc, (days)
u	=	velocity radial component, (km/s)
V	=	E-sail grid electric voltage, (kV)
V_i	=	ions electric potential, (kV)
v	=	velocity circumferential component, (km/s)
α	=	pitch angle, (deg)
α_λ	=	primer vector angle, (deg)
γ	=	gamma distribution

*Ph.D. student, Department of Civil and Industrial Engineering, via G. Caruso 8, Pisa.
†Research assistant, Department of Civil and Industrial Engineering, via G. Caruso 8, Pisa.
‡Professor, Department of Civil and Industrial Engineering, via G. Caruso 8, Pisa.
§Professor, Department of Civil and Industrial Engineering, via G. Caruso 8, Pisa.

ϵ_0	=	vacuum permittivity, (F/m)
θ	=	polar angle, (rad)
$\hat{\boldsymbol{\theta}}$	=	circumferential unit vector
$\boldsymbol{\lambda_v}$	=	primer vector
$\lambda_r, \lambda_\theta, \lambda_u, \lambda_v$	=	adjoint variables
$\mu_\odot$	=	Sun's gravitational parameter, (km^3/s^2)
$\sigma_\oplus$	=	maximum thrust per unit of tether length, (N/m)
τ	=	switching parameter
ω	=	longitude of pericenter, (rad)

Subscripts

0	=	value at initial time
f	=	value at final time
max	=	maximum allowable value

Superscripts

$\cdot$	=	time derivative
$-$	=	nominal design value
$*$	=	optimal value

1. Introduction

An Electric Solar Wind Sail (E-sail) is an innovative propellantless propulsion system able to generate the propulsive thrust by exchanging momentum with the solar wind charged particles. The E-sail heliocentric trajectory is often analyzed in an optimal framework by looking for the optimal control law that minimizes the total time of flight required to reach a target celestial body [1, 2]. In a preliminary mission analysis phase, the E-sail thrust is usually modelled by assuming an average value of the solar wind characteristics. The latter, however, are subject to non-negligible variations over time [3] and, indeed, recent simulations suggest to describe the E-sail propulsive acceleration as a stochastic variable rather than a deterministic one, as discussed by Niccolai et al. [4].

A quantification of the effects of uncertainties on aircraft and spacecraft trajectory planning is a critical issue, which has been extensively investigated in the literature [5]. In a recent work by Greco et al. [6], an extension of a direct multiple-shooting method is introduced to deal with optimal control problems in the presence of uncertainties. Ross et al. [7] defined a Lebesgue-Stieltjes optimal control problem to compute an open-loop control law able to steer a spacecraft toward a final, target state in uncertain environments. Sun et al. [8] proposed a combination of differential algebra and Gaussian mixture model method for uncertainty propagation, which was shown to be able to capture possible non-Gaussianity in uncertainty propagation through non-linear dynamics. Niccolai et al. [4] proposed to account for the solar wind fluctuations by modelling the dynamic pressure as a random variable with gamma probability density function (PDF). They also showed, using a simple test case with a Sun-facing sail, that the uncertainty in the spacecraft state is non-negligible even after one half revolution around the Sun only. This means that the spacecraft cannot be steered toward a target state in an uncertain environment, by means of an open-loop control law. The proposed solution for that problem was the introduction of a control law aimed at adjusting the E-sail grid voltage in response to the dynamic pressure fluctuations (measured by a sensor onboard the spacecraft), in such a way to maintain the E-sail propulsive characteristics equal to a given design value. However, due to the limitation in the maximum allowable value of the grid electric voltage, the spacecraft may not be able to follow the nominal optimal reference trajectory.

This paper proposes a possible solution for such a problem. In essence, the idea is to generate a new control law which steers the spacecraft toward the target orbit as soon as the spacecraft departs from the nominal reference trajectory. The new rectified trajectory is calculated by solving an optimal problem with an indirect approach. The paper is organized as follows. The next section introduces the mathematical model used to compute the E-sail trajectory. Section 3 describes the indirect method that generates the initial nominal reference trajectory. Then, a rectification method is introduced, which is finally applied in Section 4 to two-dimensional cases involving Earth-Mars and Earth-Apophis transfers.

2. Problem description

Consider an E-sail based spacecraft that initially covers a heliocentric elliptic orbit of semilatus rectum p_0 and eccentricity e_0. The mission aim is to transfer the spacecraft to a coplanar, target orbit of semilatus rectum p_f, eccentricity e_f and longitude of pericenter $\omega_f \in [0, 2\pi)$ rad, the latter being the angle between the Sun-pericenter line of the two orbits measured counterclockwise from the initial one; see Fig. 1.

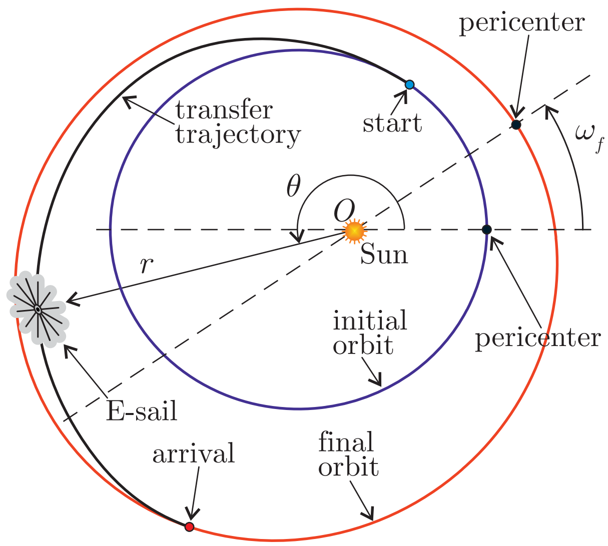

Fig. 1 Geometry of the problem.

The heliocentric motion of the spacecraft is conveniently described by introducing a polar reference frame $\mathcal{T}(O;\, r, \theta)$, where O is the Sun's center-of-mass, r is the Sun-spacecraft distance, and θ is the polar angle measured counterclockwise from the Sun-pericenter direction of the initial orbit; see also Fig. 1. The spacecraft equations of motion in $\mathcal{T}$ are

$$\dot{r} = u \tag{1}$$

$$\dot{\theta} = \frac{v}{r} \tag{2}$$

$$\dot{u} = -\frac{\mu_\odot}{r^2} + \frac{v^2}{r} + a_r \tag{3}$$

$$\dot{v} = -\frac{u\,v}{r} + a_\theta \tag{4}$$

where the dot symbol denotes a derivative taken with respect to time, u and v are the radial and circumferential components of the spacecraft velocity, $\mu_\odot \simeq 132\,712\,439\,935\,\mathrm{km}^3/\mathrm{s}^2$ is the Sun's gravitational parameter, while a_r and a_θ are the components of the E-sail propulsive acceleration along the radial (with unit vector $\hat{\boldsymbol{r}}$) and circumferential (with unit vector $\hat{\boldsymbol{\theta}}$) directions, respectively.

Using the recent model proposed by Huo et al. [9], the propulsive acceleration vector $\boldsymbol{a}$ for a flat and axially-symmetric E-sail can be written as

$$\boldsymbol{a} = \tau \frac{a_c}{2} \frac{r_\oplus}{r} \left[\hat{\boldsymbol{r}} + (\hat{\boldsymbol{r}} \cdot \hat{\boldsymbol{n}})\hat{\boldsymbol{n}}\right] \tag{5}$$

where $\tau \in \{0, 1\}$ is a variable that models the possibility of switching the electron gun either on ($\tau = 1$) or off ($\tau = 0$), and $\hat{\boldsymbol{n}}$ is the normal to the E-sail nominal plane in the direction opposite to the Sun. In Eq. (5), a_c is the characteristic acceleration, defined as the maximum propulsive acceleration magnitude provided by the E-sail at a distance $r_\oplus = 1$ au $\simeq 149\,597\,870$ km from the Sun, and given by [9]

$$a_c = \frac{N L \sigma_\oplus}{m} \tag{6}$$

where N and L are the number of tethers and their length, respectively, and m is the total spacecraft mass. The thrust per unit of tether length generated by the E-sail at a distance $r \simeq r_\oplus$ is

$$\sigma_\oplus = 0.18 \max(0, V - V_i)\sqrt{\epsilon_0 p_\oplus} \tag{7}$$

where ϵ_0 is the vacuum permittivity, $p_\oplus$ is the dynamic pressure of the solar wind measured at a distance $r = r_\oplus$, V is the E-sail grid voltage, and V_i is the electric potential of the ions. Because V is usually on the order of some tens of kV, that is, much larger than V_i (which is about 1 kV), the components of the propulsive acceleration along the radial and circumferential directions are

$$a_r = \boldsymbol{a} \cdot \hat{\boldsymbol{r}} = \tau \, \frac{0.18NLV}{2m} \sqrt{\epsilon_0 p_\oplus} \, \frac{r_\oplus}{r} \left(1 + \cos^2 \alpha\right) \tag{8}$$

$$a_\theta = \boldsymbol{a} \cdot \hat{\boldsymbol{\theta}} = \tau \, \frac{0.18NLV}{2m} \sqrt{\epsilon_0 p_\oplus} \, \frac{r_\oplus}{r} \, \cos\alpha \sin\alpha \tag{9}$$

where $\alpha \in [-90, 90]$ deg is the pitch angle, defined as the angle between $\hat{\boldsymbol{r}}$ and $\hat{\boldsymbol{n}}$; see Fig. 2.

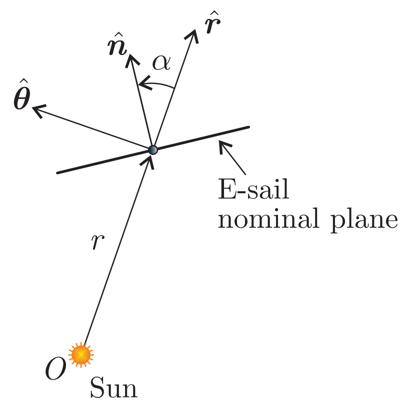

Fig. 2 Definition of pitch angle α.

In a preliminary mission analysis phase, the E-sail heliocentric transfer trajectory is typically calculated by assuming an average value of the solar wind characteristics. In particular, the value of $p_\oplus$ is taken as constant and equal to its mean value, $\bar{p}_\oplus = 2$ nPa. In that case, when the control law $\{\tau, \alpha\}$ is known, the spacecraft trajectory may be obtained through a numerical integration of the equations of motion (1)-(4), starting from the initial conditions associated to an elliptic orbit, that is

$$r(t_0) = \frac{p_0}{1 + e_0 \cos\theta_0} \tag{10}$$

$$u(t_0) = \sqrt{\frac{\mu_\odot}{p_0}} e_0 \sin\theta_0 \tag{11}$$

$$v(t_0) = \sqrt{\frac{\mu_\odot}{p_0}} \left(1 + e_0 \cos\theta_0\right) \tag{12}$$

where $t_0 \triangleq 0$ is the initial time, and $\theta_0 \in [0, 2\pi)$ rad is the polar angle at departure, which coincides with the spacecraft true anomaly along the initial orbit.

A more reliable analysis, however, requires the effects of the solar wind uncertainties on the spacecraft trajectory to be taken into account. Because in this work two-dimensional transfers are assumed, the possible variations of $p_\oplus$ with the latitude are not taken into account [10]. As is well known, the solar wind properties are subject to non negligible variations over time [3]. For example, Fig. 3 shows the hourly fluctuations of the solar wind dynamic pressure at a Sun-spacecraft distance of 1 au, in a time span from January 1996 to September 2013. These data suggest the E-sail propulsive acceleration to be handled as a stochastic variable rather than a deterministic one. This is indeed the approach

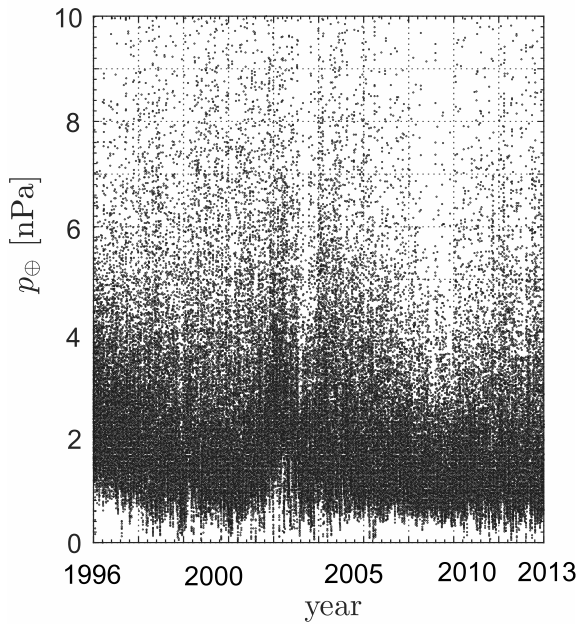

Fig. 3 Hourly variation of $p_\oplus$ from January 1996 to September 2013; data from NASA.

pursued by Niccolai et al. [4], who suggested to model the dynamic pressure as a random variable with a gamma distribution, in the form

$$\gamma(p_\oplus) = \frac{p_\oplus^{A-1}}{B^A \Gamma(A)} \exp\left(-p_\oplus/B\right) \tag{13}$$

with parameters $A = 1.6437$ and $B = 1.2168$. The probability density function of $p_\oplus$ is shown in Fig. 4.

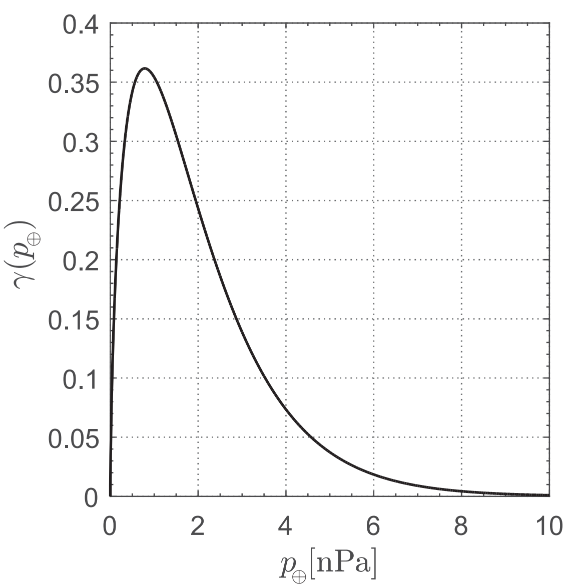

Fig. 4 Probability density function of $p_\oplus$. Figure adapted from Ref. [4]

The following section proposes a possible procedure to investigate optimal (minimum-time) E-sail transfer trajectories that takes into account the uncertainties on the solar dynamic pressure.

3. Trajectory optimization

The heliocentric transfer problem of an E-sail-based spacecraft is usually studied within an optimal framework, by looking for the optimal control law $\{\tau^*, \alpha^*\}$ that minimizes the total mission time t_f. As long as $p_\oplus$ is taken constant and equal to its mean value $\bar{p}_\oplus = 2\,\mathrm{nPa}$, the E-sail characteristic acceleration has a constant value given by [4]

$$\bar{a}_c = \frac{0.18 N L \bar{V}}{m} \sqrt{\epsilon_0 \bar{p}_\oplus} \tag{14}$$

where $\bar{V}$ is the nominal design value of the grid electric voltage. The resulting optimization problem is therefore deterministic, and amounts to maximizing the performance index

$$J = -t_f \tag{15}$$

subject to the equations of motion (1)-(4) and to the boundary constraints at the initial time (given by Eqs (10)-(12)) and at the final time

$$r(t_f) = \frac{p_f}{1 + e_f \cos(\theta_f - \omega_f)} \tag{16}$$

$$u(t_f) = \sqrt{\frac{\mu_\odot}{p_f}} e_f \sin(\theta_f - \omega_f) \tag{17}$$

$$v(t_f) = \sqrt{\frac{\mu_\odot}{p_f}} \left(1 + e_f \cos(\theta_f - \omega_f)\right) \tag{18}$$

where θ_f is the polar angle at t_f. Note that both the values of θ_0 and θ_f are left unconstrained. This problem may be solved with an indirect method [1, 11]. To that end, introduce the adjoint functions λ_r, λ_θ, λ_u and λ_v associated to the state variables r, θ, u and v, respectively. The corresponding Hamiltonian function is

$$\mathcal{H} = \lambda_r u + \lambda_\theta \frac{v}{r} + \lambda_u \left(-\frac{\mu_\odot}{r^2} + \frac{v^2}{r} + a_r\right) + \lambda_v \left(-\frac{u\,v}{r} + a_\theta\right) \tag{19}$$

and, using the Euler-Lagrange equations [11], the derivatives of the adjoint variables are

$$\dot{\lambda}_r = -\frac{\partial \mathcal{H}}{\partial r} = \lambda_\theta \frac{v}{r^2} + \lambda_u \left(\frac{v^2}{r^2} - \frac{2\mu_\odot}{r^3} + \frac{a_r}{r}\right) + \lambda_v \left(-\frac{uv}{r^2} + \frac{a_\theta}{r}\right) \tag{20}$$

$$\dot{\lambda}_\theta = -\frac{\partial \mathcal{H}}{\partial \theta} = 0 \tag{21}$$

$$\dot{\lambda}_u = -\frac{\partial \mathcal{H}}{\partial u} = -\lambda_r + \lambda_v \frac{v}{r} \tag{22}$$

$$\dot{\lambda}_v = -\frac{\partial \mathcal{H}}{\partial v} = -\frac{\lambda_\theta}{r} - 2\lambda_u \frac{v}{r} + \lambda_v \frac{u}{r} \tag{23}$$

where a_r and a_θ are given by Eqs. (8)-(9), with $p_\oplus = \bar{p}_\oplus$ and $V = \bar{V}$.

According to Ref. [9], the optimal control law that maximizes the Hamiltonian function at each time instant is

$$\tau^* = \frac{1 + \operatorname{sign}(1 + 3\cos\alpha_\lambda)}{2} \tag{24}$$

$$\alpha^* = \frac{\alpha_\lambda}{2} \tag{25}$$

where $\operatorname{sign}(\cdot)$ is the signum function, whereas $\alpha_\lambda \in [-180, 180]\,\mathrm{deg}$ is the angle between $\hat{\boldsymbol{r}}$ and $\boldsymbol{\lambda_v} = [\lambda_u, \lambda_v]^{\mathrm{T}}$, the latter being the Lawden's primer vector [12].

The minimum time trajectory is the solution of a two-point boundary value problem (TPBVP), constituted by the equations of motion (1)-(4), the Euler-Lagrange equations (20)-(23), with initial boundary conditions (10)-(12), final boundary conditions (16)-(18), and transversality conditions [11]

$$\lambda_\theta(t_0) = -\lambda_r(t_0)\frac{p_0 e_0 \sin\theta_0}{(1+e_0\cos\theta_0)^2} - \lambda_u(t_0)\sqrt{\frac{\mu_\odot}{p_0}}e_0\cos\theta_0 + \lambda_v(t_0)\sqrt{\frac{\mu_\odot}{p_0}}e_0\sin\theta_0 \tag{26}$$

$$\lambda_\theta(t_f) = -\lambda_r(t_f)\frac{p_f e_f \sin(\theta_f-\omega_f)}{(1+e_f\cos(\theta_f-\omega_f))^2} - \lambda_u(t_f)\sqrt{\frac{\mu_\odot}{p_f}}e_f\cos(\theta_f-\omega_f) + \lambda_v(t_f)\sqrt{\frac{\mu_\odot}{p_f}}e_f\sin(\theta_f-\omega_f) \tag{27}$$

$$\mathcal{H}(t_f) = 1 \tag{28}$$

The solution to such a TPBVP coincides with the reference trajectory that would be tracked by the spacecraft in the nominal case, when $p_\oplus = \bar{p}_\oplus$. However, the uncertainties on the actual value of the solar wind dynamic pressure prevent the spacecraft to reach the target state. This problem may be solved with the aid of a control law that suitably adjusts the tether voltage, as is now shown.

3.1 Reference trajectory rectification

Niccolai et al. [4] suggested a possible control strategy to track the nominal trajectory in the presence of dynamic pressure fluctuations. Under the assumption that the spacecraft is able to measure the local value of the solar wind dynamic pressure $p(t)$, the grid electric voltage V is adjusted [4] in such a way that the characteristic acceleration meets its nominal value $\bar{a}_c$; see Eq. (14). The required value of the grid voltage is therefore

$$V_{\text{req}} = \frac{m\bar{a}_c}{0.18NL\sqrt{\epsilon_0 p_\oplus(t)}} \tag{29}$$

with $p_\oplus(t) = p(t)\,(r/r_\oplus)^2$. Because $V(t)$ cannot exceed a maximum value $V_{\max}$, the control law is defined as

$$V(t) = \begin{cases} V_{\text{req}}(t) & \text{if} \quad V_{\text{req}}(t) < V_{\max} \\ V_{\max} & \text{if} \quad V_{\text{req}}(t) \geq V_{\max} \end{cases} \tag{30}$$

Note that the control variables τ and α are exactly the same as those in the nominal case (that is, obtained by solving the previous TPBVP). Also note that, as long as $\tau = 0$, the spacecraft trajectory presents a Keplerian arc. In that case, there is no need to use the control law (30) because, as the E-sail thrust is off, the spacecraft covers the reference trajectory for any value of $p_\oplus$.

The whole reference trajectory (calculated with $p_\oplus = \bar{p}_\oplus$) is first partitioned into a certain number of arcs. Within each arc, the value of the solar wind dynamic pressure is maintained constant and equal to that randomly generated with a gamma distribution (13), while the grid voltage is varied in accordance with Eqs. (29)-(30). As long as $V_{\text{req}} < V_{\max}$, the characteristic acceleration along the arc is equal to its nominal value $\bar{a}_c$, and the spacecraft is able to track the nominal optimal trajectory. However, when the dynamic pressure becomes very small, the grid voltage V_{req} needs to much increase its value to generate a sufficient thrust, with a possible saturation problem (in that case, according to Eq. (30), the grid voltage is set equal to $V_{\max}$). Along such an arc, the E-sail characteristic acceleration is less than its nominal value, that is, $a_c < \bar{a}_c$, which induces the spacecraft to leave its reference trajectory. At the end of such an arc (referred to as deviation arc), the state vector is therefore different from its nominal value; see Fig. 5.

This problem may be circumvented by a rectification of the reference trajectory. This amounts to generating a new optimal trajectory (starting from the spacecraft state at the end of a deviation arc), which steers the spacecraft toward the final orbit, as is shown in Fig. 5, assuming again a constant value of $p_\oplus = \bar{p}_\oplus$. Accordingly, a new optimal control problem arises, in which the performance index to maximize is

$$J_{\text{corr}} = -\left(t_f - t^{\text{d}}_{\text{end}}\right) \tag{31}$$

where $t^{\text{d}}_{\text{end}}$ is the initial time along the new reference trajectory, which coincides with the time at the end of the deviation arc. The spacecraft initial conditions are

$$r\left(t^{\text{d}}_{\text{end}}\right) = r^{\text{d}}_{\text{end}}, \quad \theta\left(t^{\text{d}}_{\text{end}}\right) = \theta^{\text{d}}_{\text{end}}, \quad u\left(t^{\text{d}}_{\text{end}}\right) = u^{\text{d}}_{\text{end}}, \quad v big(t^{\text{d}}_{\text{end}}\right) = v^{\text{d}}_{\text{end}} \tag{32}$$

where $\{r^{\text{d}}_{\text{end}}, \theta^{\text{d}}_{\text{end}}, u^{\text{d}}_{\text{end}}, v^{\text{d}}_{\text{end}}\}$ is the state of the spacecraft at the end of the deviation arc. The final boundary conditions are the same as those expressed by Eqs. (16)-(18), where θ_f is again left unconstrained. The spacecraft is subject to the

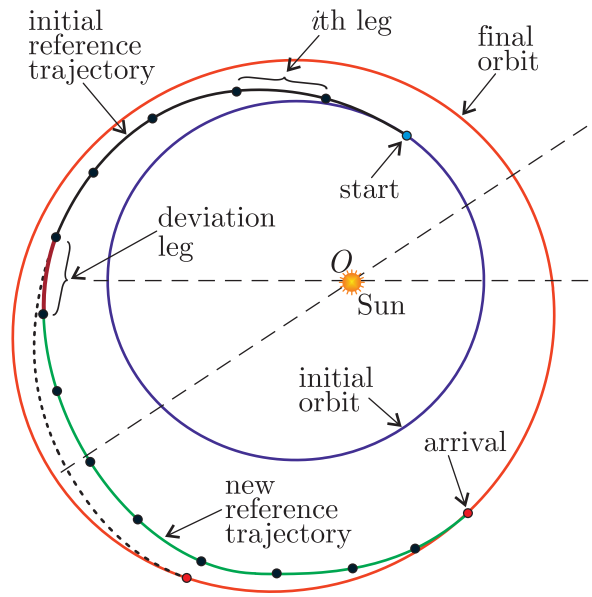

Fig. 5 Deviation arc and generation of the new reference trajectory.

dynamical equations (1)-(4), and to the Euler-Lagrange equations (20)-(23). The resulting TPBVP is completed by the transversality conditions (27)-(28). Note that, in this case, the value of λ_θ at the initial time $t^{\mathrm{d}}_{\mathrm{end}}$ is unconstrained.

The solution to such a TPBVP gives a new reference trajectory (and a new optimal control law $\{\tau^*, \alpha^*\}$), which is tracked by the spacecraft from $t = t^{\mathrm{d}}_{\mathrm{end}}$ until a new deviation arc arises, when $a_c < \bar{a}_c$. The previous procedure is repeated until the spacecraft reaches the final, target orbit.

4. Numerical simulations

In this section some numerical examples are given, where the optimal transfer trajectory is obtained taking into account the presence of uncertainties in the solar wind dynamic pressure. An Earth-Mars and an Earth-Apophis transfer are investigated using the method described in the previous section. In particular, the equations of motion (1)-(4) and the Euler-Lagrange equations (20)-(23) are integrated by means of a variable-step Adams-Bashforth-Moulton solver scheme [13, 14] with absolute and relative errors of 10^{-12}.

In the following discussion, the spacecraft is propelled by an E-sail with a total number of tethers $N = 62$, each one of length $L = 19.4$ km. The nominal grid voltage is 25 kV, and the total spacecraft mass is about $m = 700$ kg [15]. Note that, in the ideal case of $p_\oplus = \bar{p}_\oplus$, such a configuration has a nominal characteristic acceleration $\bar{a}_c = 1\,\mathrm{mm/s^2}$.

4.1 Earth-Mars transfer

An Earth-Mars transfer is first analyzed, assuming the orbit of both Earth and Mars to be coplanar. Therefore, the spacecraft initially covers an orbit coincident with that of the Earth (with $p_0 = 1$ au and $e_0 = 0.0167$), and it has to be transferred to a final orbit coinciding with that of Mars ($p_f = 1.524$, $e_f = 0.0934$, and $\omega_f = 233.1$ deg).

The nominal optimal trajectory (in the case of $p_\oplus = \bar{p}_\oplus$) is first computed, and the total transfer time is found to be 465.37 days. The whole trajectory is then partitioned into 1800 arcs, each one with a length of about 6.2 hours, and a maximum grid voltage $V_{\max} = 80$ kV is assumed. Along each arc, a value of $p_\oplus$ is generated with a gamma PDF (13), and each time the required grid voltage V_{req} exceeds $V_{\max}$, the spacecraft trajectory deviates from the nominal optimal one and a reference trajectory rectification is obtained by computing a new reference path and the corresponding control law that steers the spacecraft toward the final orbit, as previously described.

At each run, a different control law is calculated, since the latter depends on the random values of $p_\oplus$ generated according to its PDF. However, the numerical simulations show no significant differences between the nominal optimal trajectory (that is, without dynamic pressure fluctuations) and the trajectory with the rectification approach (which instead accounts for uncertainties), with a small increase in the total flight time, on the order of a few tens of hours only. An example is shown in Fig. 6, where the flight time increase is about $\Delta t_{\rm inc} = 25.32$ hours. Figures 7-8 also show the

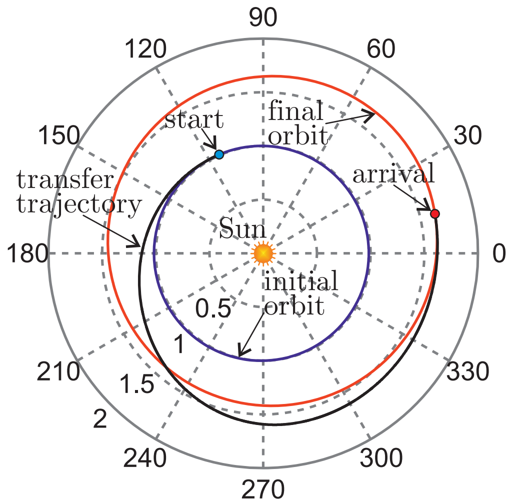

Fig. 6 Optimal Earth-Mars trajectory.

optimal control law $\{\tau^*, \alpha^*\}$ in both cases with (black line) or without (red line) uncertainties in the value of $p_\oplus$. Note that even though a small deviation of the optimal value of α^* arises, the optimal control τ^* in both cases is the same.

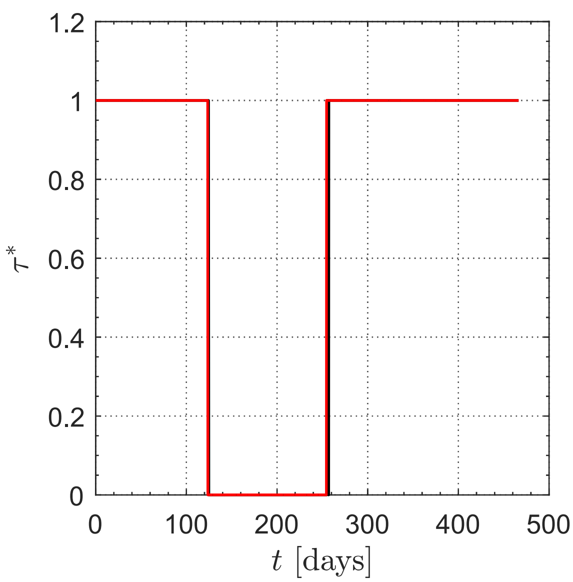

Fig. 7 Earth-Mars transfer: optimal control law τ^* in the case with uncertainties in the value of $p_\oplus$ (black line), and in the nominal case of constant $p_\oplus = \bar{p}_\oplus$ (red line).

4.2 Transfer toward asteroid 99942 Apophis

Consider now a transfer toward the asteroid 99942 Apophis. Again, the spacecraft initial orbital parameters are $p_0 = 1$ au and $e_0 = 0.0167$. The orbital inclination of Apophis with respect to the ecliptic plane (about 3.3 deg) is

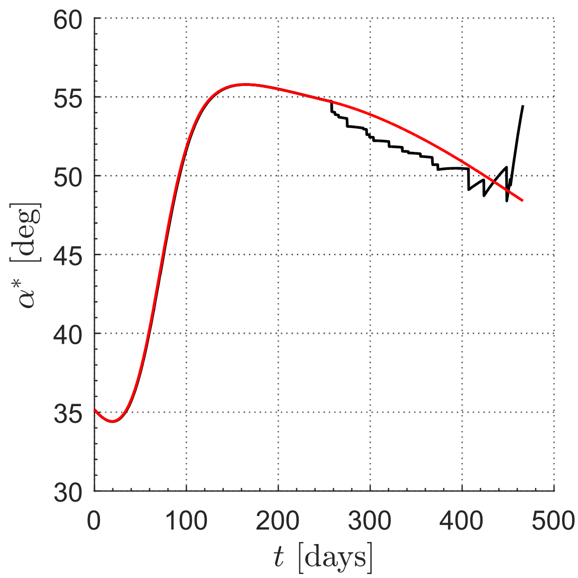

Fig. 8 Earth-Mars transfer: optimal control law α^* in the case of uncertainties in the value of $p_\oplus$ (black line), and in the nominal case of constant $p_\oplus = \bar{p}_\oplus$ (red line).

neglected, while the other orbital parameters are $a_f = 0.8891$ au, $e_f = 0.1912$ and $\omega_f = 227.9$ deg.

The transfer time along the optimal nominal trajectory is 83.1 days. The trajectory is then partitioned into 300 arcs of about 6.6 hours each. The optimal trajectory is shown in Fig. 9, while Figs. 10-11 show the effect of the uncertainties on the optimal control law. In this example, the time increment is $\Delta t_{\text{inc}} = 11.39$ hours. Again, no substantial differences

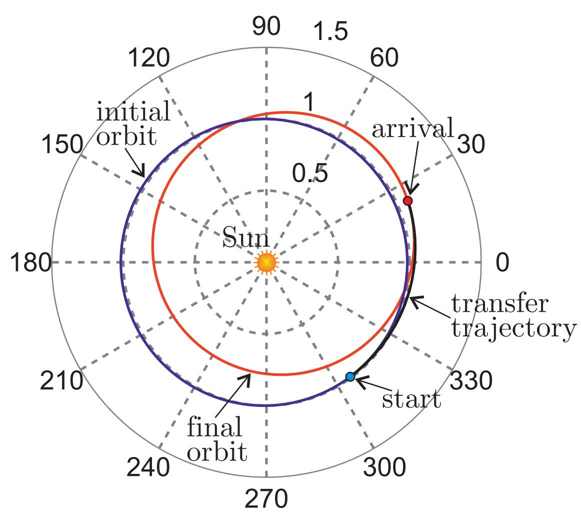

Fig. 9 Optimal Earth-Apophis trajectory.

can be observed in both the trajectory and the control law τ^*, whereas the value of α^* deviates from the nominal one to steer the spacecraft towards the target orbit.

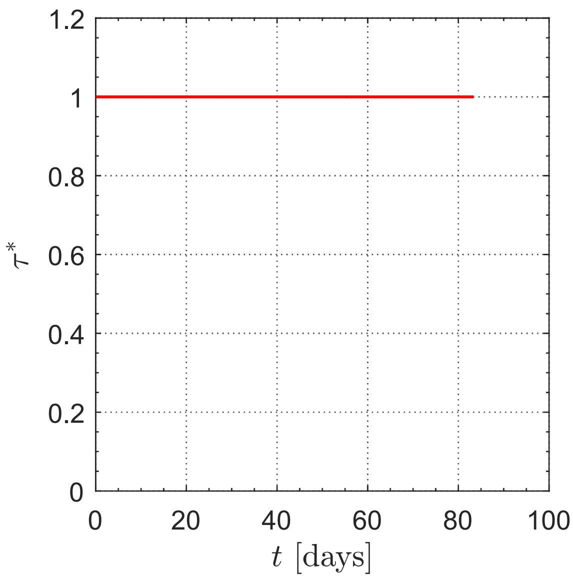

Fig. 10 Earth-Apophis transfer: optimal control law τ^* in the case of uncertainties in the value of $p_\oplus$ (black line), and in the nominal case of constant $p_\oplus = \bar{p}_\oplus$ (red line).

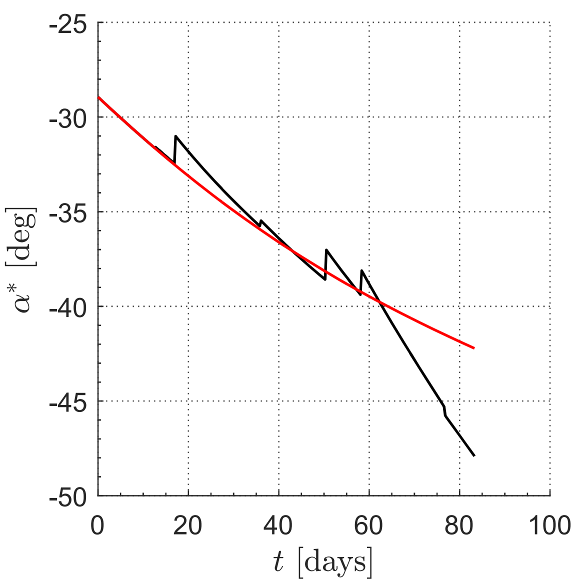

Fig. 11 Earth-Apophis transfer: optimal control law α^* in the case with uncertainties in the value of $p_\oplus$ (black line), and in the nominal case of constant $p_\oplus = \bar{p}_\oplus$ (red line).

5. Conclusion

This work has proposed a possible strategy to generate an optimal trajectory to transfer an E-sail based spacecraft from a parking orbit toward a final, elliptic orbit, while taking into account the uncertainties in the solar wind dynamic pressure. Assuming the spacecraft to be able to measure the instantaneous value of the local solar wind dynamic pressure, the grid voltage is varied such that the characteristic acceleration equals its nominal design value. Since the grid electric voltage cannot exceed a maximum allowable value, as long a saturation occurs, the spacecraft departs from its nominal trajectory, and a course correction is necessary for the spacecraft to reach the target orbit. Every time such a deviation from the reference trajectory takes place, the control law that steers the spacecraft toward the final orbit is updated, and a new reference trajectory is generated. From the numerical simulations, a minor increase in the time of flight is observed when compared to the nominal optimal trajectory, while a small pitch angle correction is sufficient for the spacecraft to reach the target orbit.

References

[1] Quarta, A. A., and Mengali, G., "Minimum-time trajectories of electric sail with advanced thrust model," *Aerospace Science and Technology*, Vol. 55, 2016, pp. 419–430. doi:10.1016/j.ast.2016.06.020.

[2] Bassetto, M., Quarta, A. A., and Mengali, G., "Locally-optimal electric sail transfer," *Proceedings of the Institution of Mechanical Engineers, Part G: Journal of Aerospace Engineering*, Vol. 233, No. 1, 2019, pp. 166–179. doi:10.1177/0954410017728975.

[3] Phillips, J. L., Bame, S. J., Barnes, A., et al., "Ulysses solar wind plasma observations from pole to pole," *Geophysical Research Letters*, Vol. 22, No. 23, 1995, pp. 3301–3304. doi:10.1029/95GL03094.

[4] Niccolai, L., Anderlini, A., Mengali, G., and Quarta, A. A., "Impact of solar wind fluctuations on Electric Sail mission design," *Aerospace Science and Technology*, Vol. 82-83, 2018, pp. 38–45. doi:10.1016/j.ast.2018.08.032.

[5] Gonzáles-Arribas, D., Soler, M., and Sanjurjo-Rivo, M., "Robust aircraft trajectory planning under wind uncertainty using optimal control," *Journal of Guidance, Control, and Dynamics*, Vol. 41, No. 3, 2018, pp. 673–688. doi:10.2514/1.G002928.

[6] Greco, C., Di Carlo, M., Vasile, M., and Epenoy, R., "An intrusive polynomia algebra multiple shooting approach to the solution of optimal control problem," *69th International Astronautical Congress (IAC)*, Bremen, Germany, 2018.

[7] Ross, I. M., Proulx, R. J., and Karpenko, M., "Unscented optimal control for orbital and proximity operations in an uncertain environment: A new zermelo problem," *AIAA/AAS Astrodynamics Specialist Conference 2014*, San Diego, CA; United States, 2014.

[8] Sun, Z. J., Luo, Y. Z., di Lizia, P., and Zazzera, F. B., "Nonlinear orbital uncertainty propagation with differential algebra and Gaussian mixture model," *Science China: Physics, Mechanics and Astronomy*, Vol. 62, No. 3, 2019. doi: 10.1007/s11433-018-9267-6.

[9] Huo, M., Mengali, G., and Quarta, A. A., "Electric sail thrust model from a geometrical perspective," *Journal of Guidance, Control, and Dynamics*, Vol. 41, No. 3, 2018, pp. 734–740. doi:10.2514/1.G003169.

[10] Sokół, J. M., Bzowski, M., Tokumaru, M., Fujiki, K., and McComas, D. J., "Heliolatitude and Time Variations of Solar Wind Structure from in situ Measurements and Interplanetary Scintillation Observations," *Solar Physics*, Vol. 285, No. 1-2, 2013, pp. 167–200. doi:10.1007/s11207-012-9993-9.

[11] Bryson, A. E., and Ho, Y. C., *Applied Optimal Control*, Hemisphere Publishing Corporation, New York, NY, 1975, Chap. 2, pp. 71–89. ISBN: 0-891-16228-3.

[12] Lawden, D. F., *Optimal Trajectories for Space Navigation*, Butterworths & Co., London, 1963, pp. 54–60.

[13] Shampine, L. F., and Gordon, M. K., *Computer Solution of Ordinary Differential Equations: The Initial Value Problem*, W. H. Freeman, San Francisco, 1975, Chap. 10.

[14] Shampine, L. F., and Reichelt, M. W., "The MATLAB ODE Suite," *SIAM Journal on Scientific Computing*, Vol. 18, No. 1, 1997, pp. 1–22. doi:10.1137/S1064827594276424.

[15] Janhunen, P., Quarta, A. A., and Mengali, G., "Electric solar wind sail mass budget model," *Geoscientific Instrumentation, Methods and Data Systems*, Vol. 2, No. 1, 2013, pp. 85–95. doi:10.5194/gi-2-85-2013.